Bizzaro et al., http://www.jcb.org/cgi/content/full/jcb.201404160/DC1

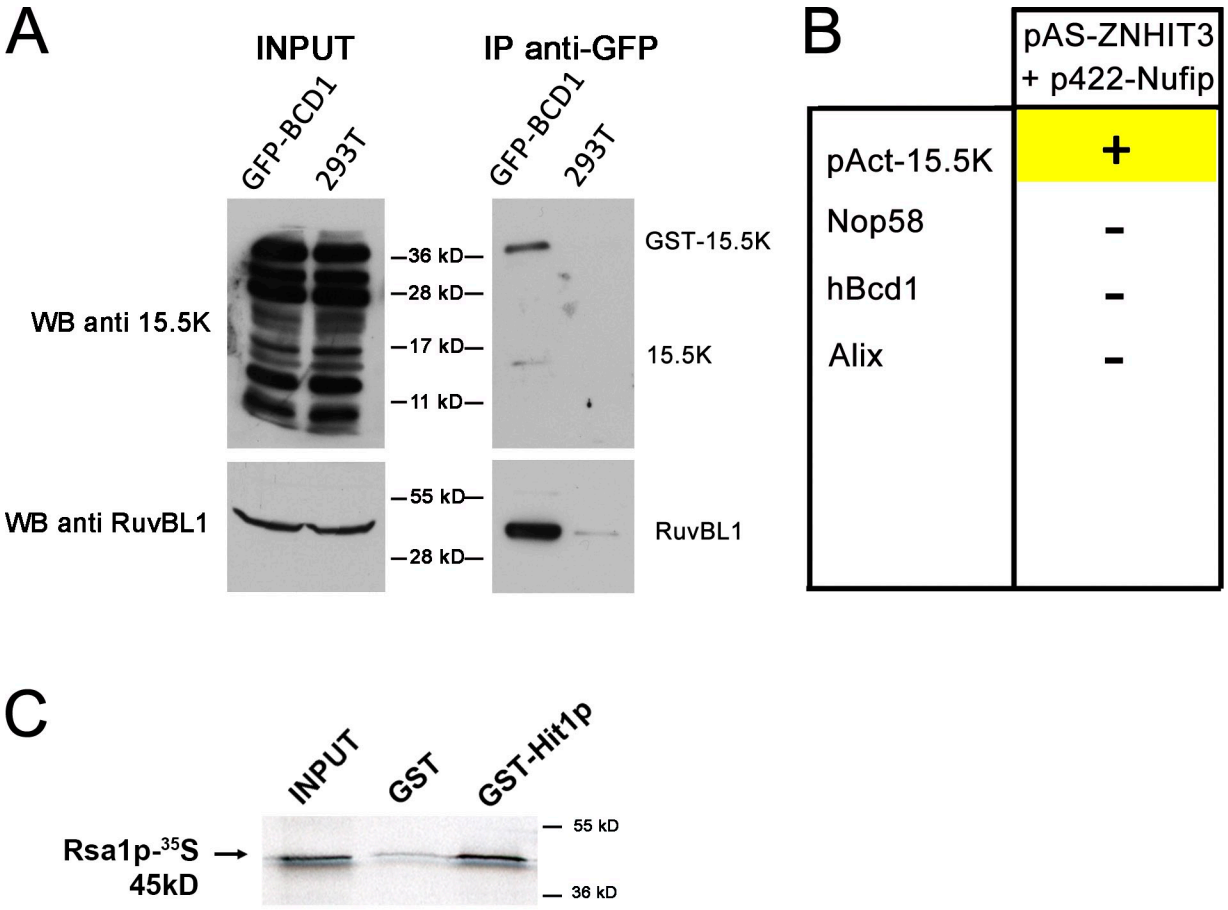

Figure S1. **Interaction between snoRNP assembly factor and C/D core proteins.** (A) Association of GFP-hBCD1 with 15.5K. 293T cells were cotransfected with vectors expressing GFP-hBCD1 and GST-15.5K. Cell extracts were immunoprecipitated with GFP-TRAP beads and analyzed by Western blots with antibodies against 15.5K and RuvBL1. (B) NUFIP mediates interaction between ZNHIT3 and 15.5K. Yeast two-hybrid assays in strains coexpressing ZNHIT3 and NUFP. Alix is used as a negative control. (C) In vitro interaction between Rsa1p and Hit1p. GST-Hit1p was produced in *E. coli* and purified on glutathione beads. Rsa1p was translated in vitro in the rabbit reticulocyte lysate with [^{35}S]methionine and tested for interaction with GST-Hit1p or GST as a control. WB, Western blot.

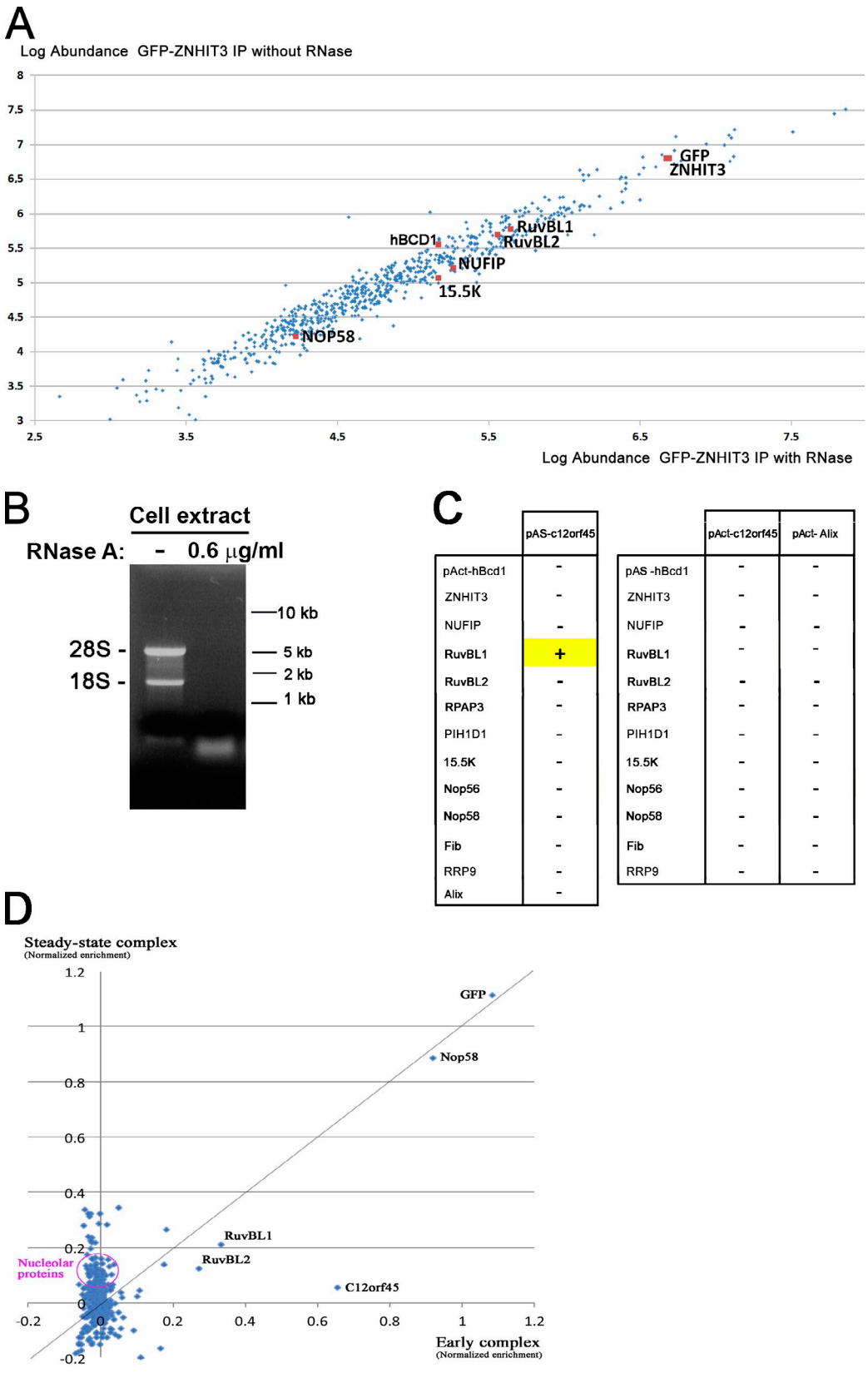

Figure S2. **RNase-independent interactions of ZNHIT3, yeast two-hybrid assay with c12orf45, and time-resolved proteomics of GFP-Nop58.** (A) RNase treatment does not disrupt the complexes purified with ZNHIT3. Extracts of GFP-ZNHIT3–expressing cells were treated or not treated with RNase and purified on GFP-TRAP beads, and pellets were analyzed by SILAC proteomics. Protein abundance in each condition was plotted against one another. (B) Effectiveness of the RNase treatment. Cell extracts were prepared in the same condition as for the proteomic experiments, and RNAs were extracted after 2 h of incubation at 4°C to mimic the incubation time with GFP-TRAP beads during real IPs. (C) Yeast strains transformed with the indicated plasmids were mated and assayed for growth on −L −T and −L −H −T selective media to test for mating and interaction, respectively. Alix is used as a negative control. Fib, Fibrillarin. (D) Time-resolved SILAC proteomic experiment. GFP-Nop58 was transiently expressed in HeLa cells for 10 h or stably expressed. These cells and control, untransfected cells were isotopically labeled and extracted by cryogrinding, GFP-Nop58 was pulled down using GFP-TRAP beads, and associated proteins were identified by MS. SILAC ratios of the specific versus control IP were normalized by first subtracting the mean ratios of all proteins identified and then by dividing by the ratio found for GFP-Nop58. X axis: early complexes (10 h of expression); y axis: steady-state complexes (stable expression).

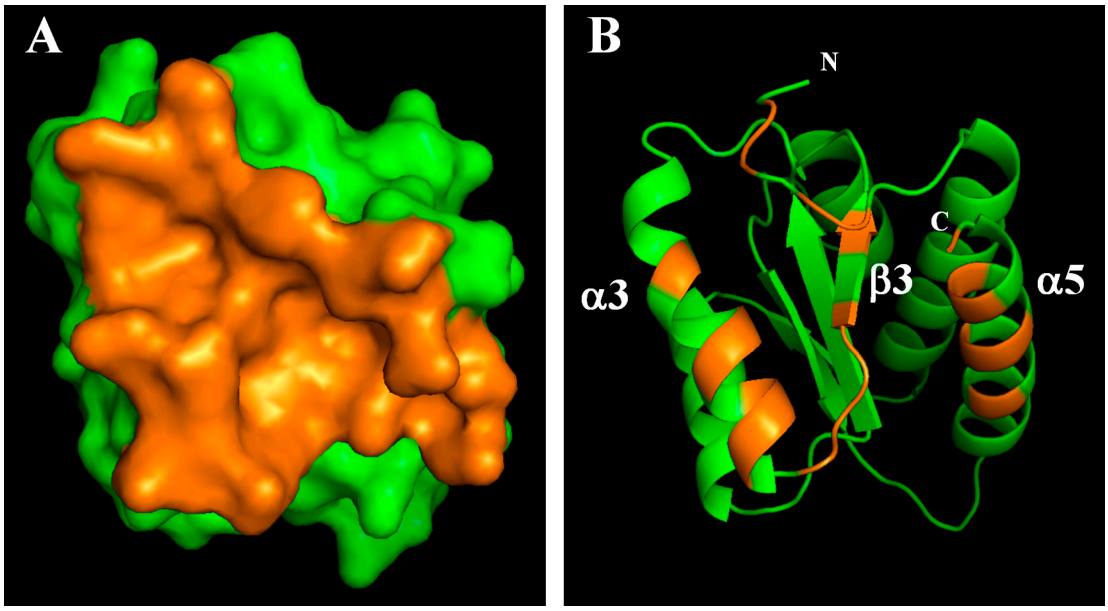

Figure S3. **A single and continuous surface of Snu13p is buried upon interaction with the PEP domain of Rsa1p.** (A and B) Solvent-accessible residues of Snu13p buried upon interaction with Rsa1p are in orange. Molecular surface (A) and ribbon representation (B) of Snu13p. A and B are in the same orientation. N, N terminal; C, C terminal.

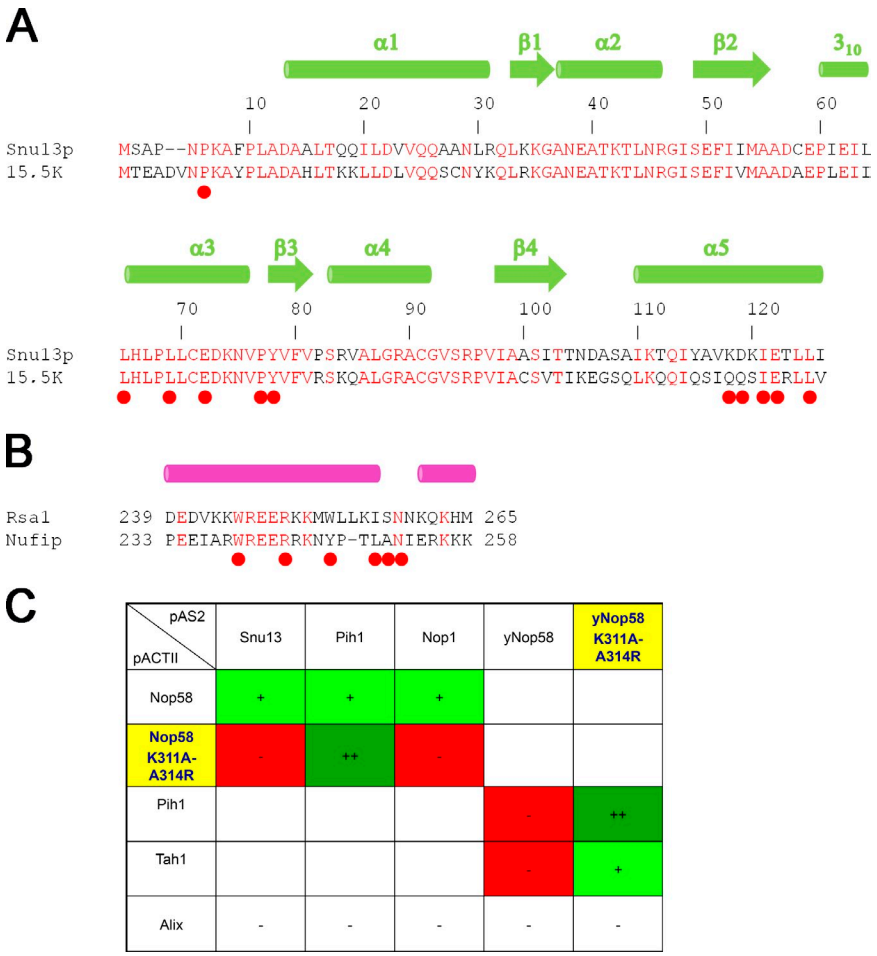

Figure S4. **Comparison of yeast Snu13p–Rsa1p with human 15.5K-NUFIP shows conservation of residues involved in the interface.** (A) Alignment of the *S. cerevisiae* Snu13p and human 15.5K protein sequences. Numbering corresponds to the *S. cerevisiae* Snu13p protein. (B) Sequence alignment of the yeast and human PEP domains in Rsa1p and NUFIP, respectively. Strictly conserved residues are in red; (−) missing residues. Secondary structure elements were assigned according to the PDB file entry. Red ovals denote the position of residues involved in the Snu13p–Rsa1p interface. (C) Yeast Nop58p mutants unable to interact with Snu13p associate more strongly with Pih1p and Tah1p. Yeast strains were transformed with two-hybrid plasmids encoding the indicated yeast proteins, mated, and tested for interaction. The Nop58p mutant K311A A314R was designed to specifically loose interaction with Snu13p, according to the crystal structure of the PRP31–15.5K–U4 complex (Liu et al., 2007). Alix is used as a negative control. Growth of 30–100% of clones on −L −T −H is scored as ++; 5–30% is scored as +; and no clones or <5% is scored as minus signs.

Table S1. **Gene nomenclature used in this study**

Human names/aliases	*S. cerevisiae* names/aliases
Nop58, Nop5	NOP58, Nop5
Nop56, Nol5A	NOP56, Sik1
Nhp2L1, Snu13, NHPX, 15.5K	SNU13
FBL, Fib, Fibrillarin	Nop1, Fibrillarin
ZNHIT6, Bcd1, c1orf181	BCD1
ZNHIT3, Trip3	HIT1
NUFIP1, Nufip	Rsa1
RuvBL1, Rvb1, Pontin, Tip49a, p55	Rvb1, Tip48, Tip49b, Tih1
RuvBL2, Rvb2, Reptin, Tip48, Tip49b, p50	Rvb2, Tip49, p50, Tih2
PIH1D1, Nop17	Pih1, Nop17
RPAP3, hSpagh	Tah1
C12orf45	–

Minus sign indicates there is no known homologue of this protein in *S. cerevisiae*.

Table S2. **Crystallographic statistics**

Datasets	Native	Se-Met
Data collection		
Space group	$P4_32_12$	$P4_32_12$
Cell parameters (Å)	a = b = 59.7, c = 92.5	a = b = 59.7, c = 92.5
Wavelength (Å)	0.980	0.979
Resolution (Å)	50.0–1.55	50.0–1.90
R_{sym} (%)[a,b]	5.7 (39.8)	5.7 (36.0)
Completeness (%)[a]	99.8 (99.5)	99.7 (99.4)
$\langle I/\sigma(I)\rangle$[a]	38.0 (5.8)	32.2 (7.7)
Multiplicity[a]	24.6 (13.1)	14.9 (14.8)
Refinement		
Resolution (Å)	40.0–1.55	
R_{factor} (%)[c]	19.6	
R_{free} (%)[d]	23.5	
r.m.s.d. bonds (Å)	0.023	
r.m.s.d. angles (°)	2.206	
Mean B values (Å^2)	26.5	
No. of protein atoms	1,169	
No. of water molecules	95	

r.m.s.d., root-mean-square deviation.
[a]Numbers in parentheses corresponds to the last resolution shell 1.55–1.63 Å and 1.90–2.00 Å for native and Se-Met data collection, respectively.
[b]$R_{sym} = \Sigma|I - \langle I\rangle|/\Sigma I$.
[c]$R_{factor} = \Sigma||F_{obs}| - |F_{calc}||/\Sigma|F_{obs}|$.
[d]For R_{free} calculation, 5% of data were selected.

Table S3 shows a hit list of the proteomic experiments and is available online as an Excel file.

Reference

Liu, S., P. Li, O. Dybkov, S. Nottrott, K. Hartmuth, R. Lührmann, T. Carlomagno, and M.C. Wahl. 2007. Binding of the human Prp31 Nop domain to a composite RNA-protein platform in U4 snRNP. *Science*. 316:115–120. http://dx.doi.org/10.1126/science.1137924